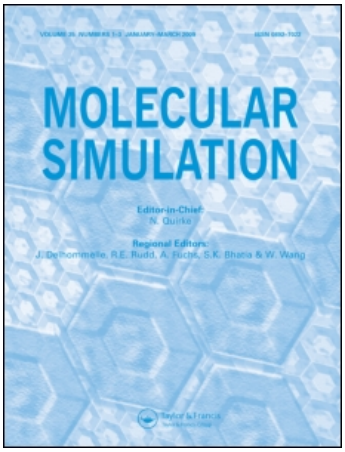

Molecular Simulation
Publication details, including instructions for authors and subscription information:
http://www.informaworld.com/smpp/title~content=t713644482

Molecular Modelling and Simulation: Tools for the Modern Era

N. Quirke[a]
[a] Department of Chemistry, Imperial College of Science, Technology and Medicine, South Kensington, United Kingdom

To cite this Article Quirke, N.(2001) 'Molecular Modelling and Simulation: Tools for the Modern Era', Molecular Simulation, 26: 1, 1 — 31
To link to this Article: DOI: 10.1080/08927020108024198
URL: http://dx.doi.org/10.1080/08927020108024198

Molecular Simulation, 2001, Vol. 26, pp. 1–31
Reprints available directly from the publisher
Photocopying permitted by license only

MOLECULAR MODELLING AND SIMULATION: TOOLS FOR THE MODERN ERA

N. QUIRKE

Department of Chemistry, Imperial College of Science, Technology and Medicine, South Kensington, SW7 2AY, United Kingdom

(Received May 2000; accepted May 2000)

Molecular simulation is an important tool for studying the physical properties of materials. In this paper computer based modelling and simulation techniques are introduced with reference to recent academic research on nanoparticle wetting and industrial applications to adsorbent design, polymer miscibility and downhole cements.

Keywords: Molecular simulation; Molecular dynamics; Metropolis Monte Carlo; Industrial applications

1. INTRODUCTION

Everything in the experienced world is a model. We hold in our consciousness a partial 'view' or 'model' sufficient to be able deal with life. For example getting out of bed involves a simple model of the mechanical properties of the floor, it will support your weight; you do not need to know all the molecular details. In this paper we define a model as a shorthand description of a complex reality. It can be qualitative (the floor is hard or soft, plastic or brittle) and/or quantitative (*e.g.*, the Rockwell scale of hardness allocates a numerical value to hardness depending on the depth reached in a standard indentation test). In scientific work the model will normally be represented mathematically.

In what follows we are interested in atomic models, those that use as a starting point, the existence of basic indivisible units, from which the materials that make up the observable universe can be constructed. The first

known model of this sort is due to Leucippus around 440BC [1]. He and his pupil, Democritus (c460-371 BC) refined and extended it in future years. There are five major points to their atomic idea.

1. All matter is composed of atoms, which are units of matter too small to be seen by eye. These atoms cannot be further split into smaller portions.
2. There is a void, which is empty space between atoms.
3. Atoms are completely solid.
4. Atoms are homogeneous, with no internal structure.
5. Atoms are different in size, shape and *weight*.

The molecular models of the type encountered in most molecular modelling software packages correspond very well to the five points of Leucippus. The major difference is that the atoms are represented mathematically and interact at a distance. The interaction between atoms is represented by a Potential Energy Surface (PES) which describes their energy as a function of the distance between them. A widely used PES (or effective potential) is the Lennard-Jones (LJ) 12–6 potential

$$V(R) = 4\varepsilon((\sigma/R)^{12} - (\sigma/R)^{6})$$

where the R^{-12} term represents electron overlap and the R^{-6} term the dispersion interaction. The parameter ε is the value of the potential minimum and σ the point at which $V(R) = 0$. The parameters are different for

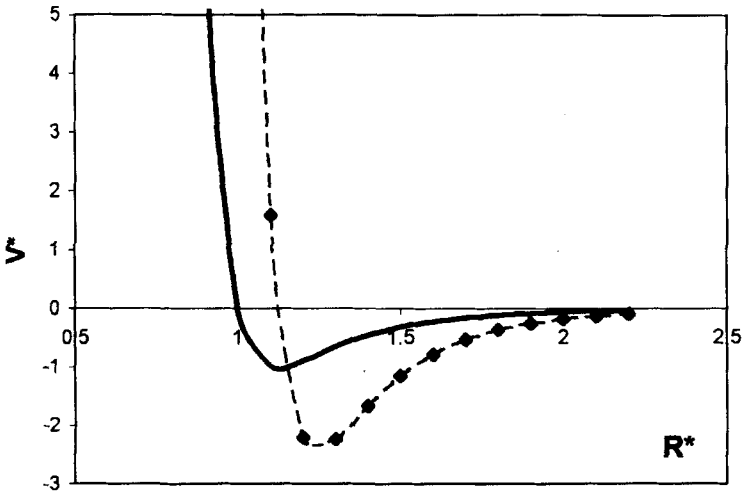

FIGURE 1 The Lennard-Jones potential in reduced units, energy $U^* = U/\varepsilon$, pair separation, $R^* = R/\sigma$. Bold line, potential, dashed, force.

different species. The force between atoms is given by

$$F_{LJ}(R) = -\partial V_{LJ}/\partial R = 24(\varepsilon/R)(2(\sigma/R)^{12} - (\sigma/R)^{6})$$

A simple effective Lennard-Jones (LJ) potential (with constant parameters ε, σ) can give a satisfactory description of the fluid phase diagram for spherical molecules and atoms and by representing each atom in a polyatomic molecule by a LJ's centre, for long chain molecules [14]. For example a diatomic molecules can be represented by an isotropic site–site LJ's plus (where appropriate) an electrostatic potential.

$$V(12) = \sum_{i=1,2}\sum_{j=1,2} 4\varepsilon((\sigma/r_{ij})^{12} - (\sigma/r_{ij})^{6}) + \sum_{l=1,N_{pc}}\sum_{m=1,N_{pc}} q_l q_m/4\pi\varepsilon_0 r_{lm}$$

where now the lower case r represents the site–site separations between LJ's sites i, j and partial charges l, m (see Fig. 2) chosen to reproduce for example the experimental electric moments of the molecule.

As an example consider the nitrogen molecule: The model effective potential requires parameters L (the bond length), ε/k_B, σ (LJ parameters) and q_l (partial charges). One possible choice (due to Cheng and Powles) is to take the bond length from X-ray data in the gas phase $L = 1.1$ A, the partial charges to reproduce the gas phase quadrupole moment $\Theta = -4.7 * 10^{-40}\,\mathrm{Cm}^2$ (see Fig. 2) and LJ's parameters $\varepsilon/k_B = 35.3$, $\sigma = 3.314$ A, from a fit (using molecular dynamics simulation discussed below) to the

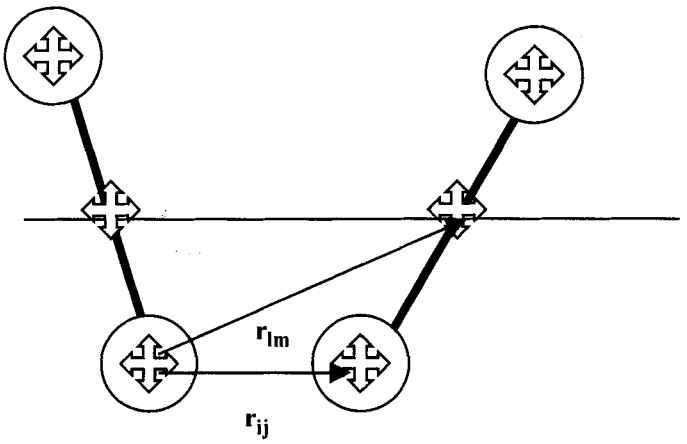

FIGURE 2 The pair interaction for diatomic molecules 1 and 2. Circles represent LJ's sites and the crosses denote the positions of partial charges.

experimental data for the internal energy and pressure of liquid nitrogen keeping $\Theta =$ constant.

Molecular modelling sometimes requires potentials that can be applied with confidence to a wide range of molecules of arbitrary complexity, and much effort has therefore been devoted to the development of potential models that account for *intramolecular* as well as intermolecular degrees of freedom, so called molecular mechanics 'forcefields'. The term forcefield is often used interchangeably with potential. Some of these more general models are limited to particular classes of molecules, such as proteins, organics or nucleic acids. The mechanical molecular model considers atoms as spheres and bonds as springs. The object of the forcefield is to predict the energy associated with a given conformation of a molecule in its electronic ground state. A simple molecular mechanics energy equation is given by:

Energy = Stretching Energy + Bending Energy + Torsion Energy + Non-Bonded Interaction Energy

These expressions together with the data (parameters) required to describe the behaviour of different kinds of atoms and bonds, are called *empirical force-field models.*

One important use of modern computers is to display molecular models graphically so that they can be viewed at different angles and various properties mapped across them. Molecular structures are commonly drawn in the form of lines representing bonds. These drawings may be referred to in different molecular graphics programs as line, stick, Dreiding, or wire-frame. In the simplest case, single lines are drawn for bonds. Another style is to add balls to represent atomic centres. Atoms are typically represented as spheres of characteristic size (*e.g.*, van der Waals diameter) in space-filling (CPK: Corey, Pauling, Koltun) models.

The molecular model can be probed by a test sphere to measure its surface properties, such as the surface area accessible to a solvent. The Van der Waals surface is the limiting surface, as probe size goes to zero, of the molecular surface. The Connolly surfaces [2] are those mapped out by probes (or solvent atoms) of different sizes as illustrated for isopentane in Figure 4.

Properties described by analytical functions or numerical data can be graphically represented in the form of contour plots. Two-dimensional or three-dimensional contours can be drawn at constant values of the function. Concentric contour surfaces can be viewed by drawing in them wire-mesh form. For example the electrostatic potential associated with the distribution of charge over the atoms of a molecule.

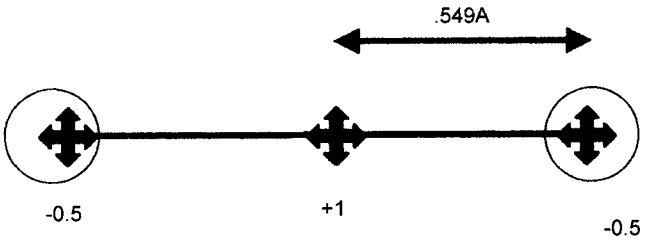

FIGURE 3 The Cheung-Powles three site partial charge (crosses) model for nitrogen. Taking $q = 16.98 * 10^{-20}$C and $l = 1.1$A gives $\Sigma q = 0$, $\mu = 0$ and $\Theta = 2q(.549 * 10^{-10})^2 = 4.7 * 10^{-40}$Cm^2.

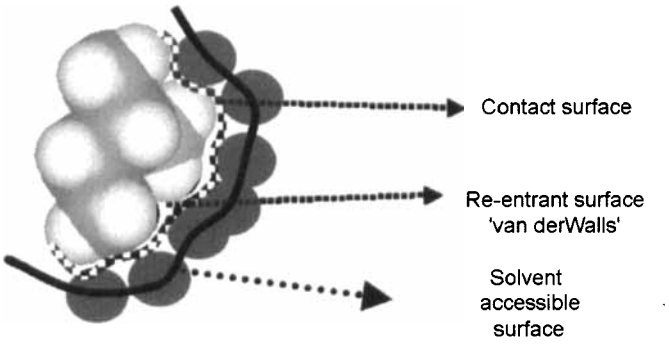

FIGURE 4 Three different ways of measuring the surface of a molecular model.

Statistical mechanics provides the link between microscopic molecular configurations and macroscopic behaviour. It allows us to introduce temperature into our modelling. There are two standard molecular modelling techniques based on statistical mechanics; molecular dynamics which solves Newton's equations of motion to obtain the trajectories (position as a function of time) of the molecules in the system, and Metropolis Monte Carlo which searches all possible configurations (positions of the molecules in space) of the system to find the most probable (*e.g.*, not those with overlapping molecules). By taking averages over these configurations (or trajectories) the properties of the system may be predicted.

The first published atomistic computer simulation was the Monte Carlo calculation of the equation of state of hard disks (the interaction between the disks is zero unless they overlap when it becomes infinite) by Metropolis *et al.* [3] which appeared in the Journal of Chemical Physics in 1953. The paper introduces all the standard concepts including importance sampling, periodic boundaries, random displacement of particles, and radial

distribution functions. They conclude that it is possible to calculate the pressure to a few percent using a few hundred particles. This is still the position for most fluid phase simulations today. A second paper [4] by the two Rosenbluths in 1954 reported the equation of state of hard spheres and some qualitative results for the two-phase region of Lennard-Jones's disks. In 1957, two letters [5, 6] appeared back to back making a comparison between Monte Carlo and *for the first time* molecular dynamics for hard spheres. The original Monte Carlo calculations had not been sufficiently equilibrated and the letters report longer calculations showing the fluid–solid phase transition region, which are now in good agreement with the molecular dynamics. Another paper by Wood and Parker the same year reports supercritical isotherms for LJ's spheres [7]. Alder and Wainwright published a full account of the molecular dynamics method for hard spheres in 1959 [8]. The first molecular dynamics calculations for a continuous potential (a Born-Mayer potential for copper) were carried out by Vineyard and colleagues studying the dynamics of radiation damage and reported in 1960 [9]. The calculation employs the familiar leapfrog algorithm. This paper is all the more significant for being the first to use the new methodology to *simulate* a real material, copper. Simulation of realistic models of liquids start in 1964 with a paper by Rahman on the correlations in the motion of atoms in liquid argon [10].

Today, molecular simulation is a vital tool in modern chemical research both for physical, inorganic and organic chemists. It also has an important role in industrial research.

2. MOLECULAR SIMULATION

The term molecular simulation [2, 11, 12, 14] refers to a group of computer based techniques that make it possible to calculate the thermodynamic, structural and transport properties of molecular models. The most common methods, Molecular Dynamics and Metropolis Monte Carlo are based on statistical mechanical procedures for correctly averaging over the molecular configurations of the system to obtain physical property data. Molecular dynamics performs time averaging and Monte Carlo, ensemble averaging. For example, a mechanical property of the system, U, such as internal energy or pressure may be expressed as a time average,

$$\langle U \rangle = \lim_{T \to \infty} 1/T \int_0^T u(t)dt$$

Or as an ensemble average

$$\langle U \rangle = \int \rho(R^n) u(R^n) dR^n$$

In each case u is a function of the microscopic positions of the n molecules, R^n. In the second equation, $\rho(R^n)$ is the probability density for finding a configuration R^n. Simulations are usually performed using a few hundred to hundreds of thousands of molecules. In order to predict the properties of bulk systems (where we may expect of the order of Avagadros number of molecules to be present) a number of special procedures are conventionally employed including periodic boundary conditions (see Fig. 5), the minimum image convention, finite range potentials and Ewald sums [2, 11, 12, 14].

In molecular dynamics the simulation algorithm follows the evolution of the molecules in time under the action of the forces between them. For atoms this can take the form due to Verlet,

$$R_i(t + \Delta t) \cong -R_i(t - \Delta t) + 2R_i(t) + (\Delta t)^2 \sum_{j \neq i} F_{ij}(t)/m_i$$

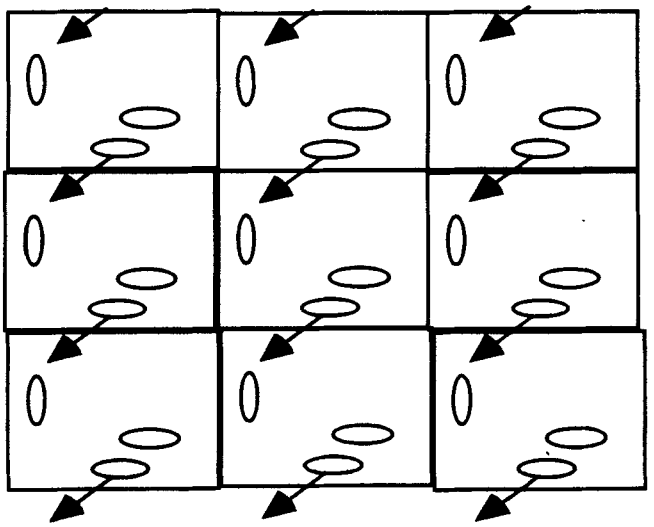

FIGURE 5 In order to simulate bulk systems with a finite number of molecules, periodic boundary conditions are employed. Only the coordinates of the molecules in the central cell are recorded, surrounding cells are filled with exact replicas. If a molecule leaves the central cell through one face, its image enters from an opposite face. The density remains constant and the effect of small system size is minimised.

where $R_i(t)$ is the position of the i'th atom at time t, Δt is an increment of time, typically 10^{-15} s, called the time step. The atomic mass is m_i. The force

$$F_{ij} = -\partial V_{ij}/\partial R_{ij}$$

is the derivative of the pair potential functions introduced earlier. The acceleration is given by

$$a_i = \sum_{j \neq i} F_{ij}(t)/m_i$$

The positions of all the particles can be estimated from a knowledge of past positions and forces. By performing many iterations of this procedure the system can be followed as it evolves in time.

A variation of the Verlet algorithm is the 'leap frog' algorithm referred to in the introduction:

$$R_i(t + \Delta t) = R_i(t) + \Delta t_i V_i(t + \Delta t/2)$$

$$V_i(t + \Delta t/2) = V_i(t - \Delta t/2) + \Delta t a_i(t)$$

The velocities at $t+\Delta t/2$ are calculated from those at $t-\Delta t/2$ and the accelerations at t. They leap frog over the velocities at t. There are many other possibilities [2, 11, 12, 14]. The choice will depend on factors such as the extent to which we require energy to be conserved for a given timestep. Molecular dynamics is most often performed in the micro-canonical ensemble for which the total energy should remain constant.

In Monte Carlo simulation we generate configurations of molecules corresponding to a given ensemble or set of external conditions. For example in the canonical ensemble we hold density and temperature constant. Each ensemble has its own probability density $\rho(R^n)$.

For the canonical ensemble we have [13]

$$\rho = \exp(-\beta V)/Z$$

where V is the energy of configuration R^n, $\beta = (1/k_B T)$, Z is the configurational partition function (a constant for the given conditions) and we approximate the integral over all space as a sum of very many configurations m of the system

$$U = \int u(R^n)\rho(R^n)dr \sim \Sigma_m u_m \rho_m$$

If we were to establish an algorithm that generated molecular configurations with a frequency ρ then

$$U \sim 1/M_c \sum_{i=1}^{M_c} u_i$$

where M_c is a large number of configurations. Properties could then be calculated from an unweighted average of the computed data. One difficulty is that we do not know Z and hence ρ cannot be computed for an arbitrary V. However an algorithm can be established from the theory of Markov chains in which it is not necessary to know Z. If one step transition probabilities for generating configuration new (n) from old (m), Π_{mn} can be found such that the condition of detailed balance

$$\rho_m \Pi_{mn} = \rho_n \Pi_{nm}$$

is obeyed then the collection of states generated by the Monte Carlo procedure will correspond to a sample from an equilibrium ensemble with probability density ρ (see for example Ref. [2]). The Metropolis algorithm has

$$\Pi_{mn} = \begin{array}{ll} \alpha_{mn} & \rho_n \geq \rho_m \\ \alpha_{mn}(\rho_n/\rho_m) & \rho_n \leq \rho_m \end{array}$$

where α_{mn} is the 'stochastic matrix' [12] representing the unweighted probability of choosing the configuration n from m.

With this choice,

$$\rho_m \alpha_{mn} = \rho_n \alpha_{nm} \frac{\rho_m}{\rho_n}$$

and microscopic reversibility is satisfied if $\alpha_{mn} = \alpha_{nm}$.

For molecular models a trial displacement can consist of a series of insertions of the constituent parts of a molecule (atoms or groups of atoms) at a new location. In densely packed molecular arrays it is possible to bias the insertions such that the accessible void space is found preferentially, saving significant simulation time. This approach, configuration bias Monte Carlo [14], weights the acceptance criterion to remove the effect of bias in the choice of trial move. For example, if $w_i^{(n)}$ is the Boltzmann weight for inserting a segment of a molecule at a trial orientation i in configuration n, then W_n is the statistical weight associated with the insertion of the whole

molecule, segment by segment:

$$W_n = \prod_{\text{segments}}^{N_{\text{seg}}} \frac{w_i^{(n)}}{\sum_{j=1}^{n_{\text{grid}}} w_j^{(n)}}$$

The new Metropolis criterion is now

$$\Pi_{mn} = \begin{array}{ll} \alpha_{mn} W_n & \rho_n \geq \rho_m \\ \alpha_{mn} W_n (\rho_n W_m / \rho_m W_n) & \rho_n \leq \rho_m \end{array}$$

$$\rho_m(\alpha_{mn} W_n) = \rho_n \alpha_{nm} W_m \left(\frac{W_n \rho_m}{W_m \rho_n} \right)$$

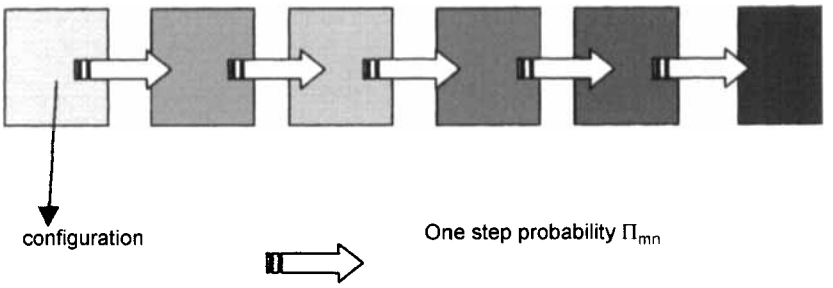

FIGURE 6 The sequence of configurations in a Markov chain.

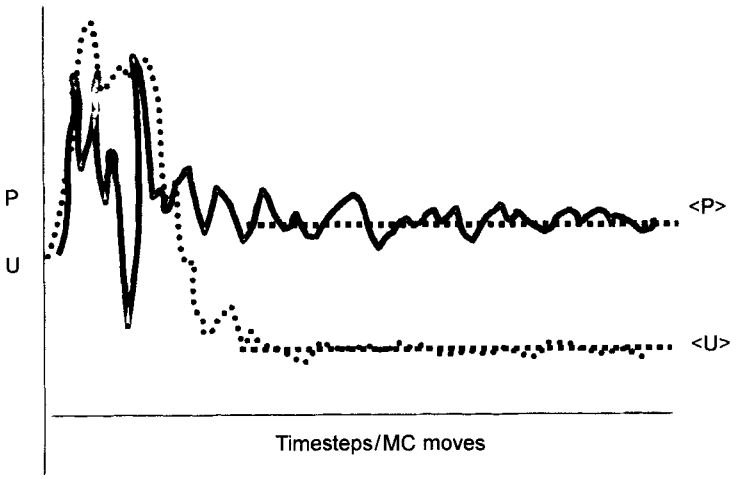

FIGURE 7 The relaxation of pressure and temperature in a typical molecular dynamics simulation, only the part of the simulation corresponding to equilibrium is used to obtain the final averages, $\langle P \rangle$ and $\langle U \rangle$.

and the condition of microscopic reversibility is satisfied, as before, if $\alpha_{mn} = \alpha_{nm}$.

A molecular simulation starts from an arbitrary initial configuration or one taken from a previous simulation on the same system. For the former case the system is unlikely to be in equilibrium. The simulation will take time to relax into an equilibrium state and these initial configurations are discarded (as indicated in Fig. 7).

In addition to standard classical molecular dynamics and Monte carlo simulations, quantum mechanical (for applications to biological systems see Ref. [15]) and mesoscale methods (see for example [16, 17]) are of increasing importance, as are mixed quantum/classical techniques [18].

3. ACADEMIC RESEARCH

In order to illustrate the use of molecular simulation in current academic research this section describes aspects of our recent work related to the physical chemistry of fluids interacting with nanostructures (nanoparticle wetting [19–21] nano-lense spreading [22], nanoparticle raft collapse [23–25], adsorption on patterned surfaces [26], phase transitions and hysterisis on surfaces and in pores [27], transport in nanopores [28], surface phonons [29], and surfactant monolayers [30]). Molecular simulation is ideally suited to study nanostructure: the length scales are now entirely accessible with modest computing facilities.

We consider the use of molecular simulation to probe the wetting of nanoparticulates. The situation of interest is displayed in Figure 8. Our aim

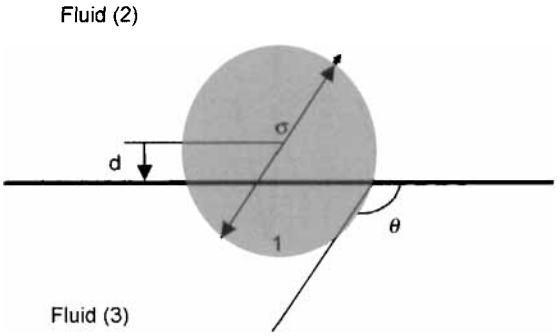

FIGURE 8 The system of interest, a particulate (labelled 1) diameter σ at a fluid interface, distance d from the fluid interface, with contact angle θ.

is to study particulates at fluid interfaces with diameters in the range one nanometre upwards to discover how they are wetted by such interfaces, what are the effects of particle size and the strength of interaction with the molecules forming the fluid interface? and whether classical models of particulate wetting such as Young's equation apply? We proceed by first defining model nanoparticulates for which there is a clear separation between the range of the interaction and the size of the particle. The particulate interacts with the Lennard-Jones atoms forming the fluid phases through a Lennard-Jones spline potential whose finite range and depth is independent of the particulate diameter (Fig. 9). Thus even for an infinite diameter, where the particulate represents a planar structureless wall, the interaction with the fluid is the same.

Using the model described above we performed molecular dynamics simulations of particulates at liquid–vapour (LV) and liquid–liquid (LL) interfaces. Figure 10 below illustrates a typical system, consisting of a liquid slab surrounded by coexisting vapour in periodic boundaries. The number of particles varied from 4000 to 24000 depending on the size of the particulate. Figure 10a shows the projection on the xy plane of the trajectory of a particulate of size $5\sigma_f$. It diffuses freely in the yz plane whilst remaining in the interface. Figure 10b depicts the x co-ordinate of the particulate as a function of time, referred to the LV equimolar dividing surface. The time average of the quantity 'd' can be related to the contact angle θ (Fig. 8) from $\cos\theta = -2d/\sigma$.

Figure 12 summarises the results [20] for the wetting properties of particulates at a LV interface as a function of size (σ/σ_f), and substrate-fluid

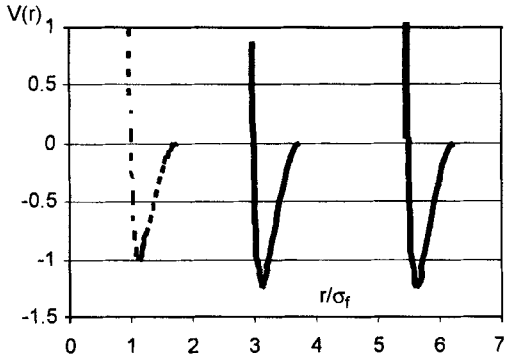

FIGURE 9 Potential models used in the simulations of particulates. From left to right, fluid–fluid interaction (LJ's spline, $\sigma_f = 1$), Particulate-fluid interaction, $\sigma = 5\sigma_f$, $\sigma = 10\sigma_f$, with $\varepsilon_P = 1.25\varepsilon_f$.

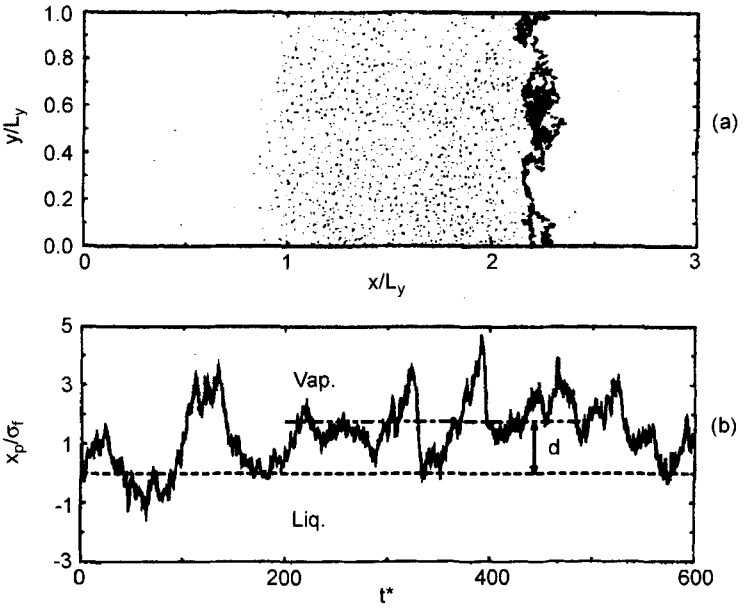

FIGURE 10 Molecular dynamics results [20] for a particle at a liquid–vapor interface, d is defined in Figure 8.

interaction ($\varepsilon/\varepsilon_f$). The wetting and drying boundaries are the points defined by the values of the contact angle, $\cos\theta = \pm 1$. The drying transition is insensitive to particulate size. The data are consistent with an increase of the wetting temperature, as the particulate becomes smaller in agreement with theoretical models. Change of size alone does not produce a completely wet state from a dry state and the region of stability in the interface narrows with decreasing σ. Small particulates are less stable in the interface than large ones and are more likely to be wet (in other words they have enhanced solubility).

The literature on line tensions reports values that differ by up to five orders of magnitude [31]. Molecular simulation offers an independent approach to the estimation of thermodynamic quantities and we have been able to compute the surface and line tensions associated with our model particulates. These data also allow an unambiguous test of Young's equation for nanoscopic interfaces

$$\cos\theta = \frac{\gamma_{12} - \gamma_{31}}{\gamma_{23}}$$

The interfacial tension γ_{23} of the planar interface was calculated in the simulations using the mechanical route *via* the difference in normal P_N and tangential pressures P_T across the planar interface (as below).

$$\gamma_{23} = \int_{x_l}^{x_v} [P_N(x) - P_T(x)]dx$$

$$P_N = \langle\rho\rangle k_B T - 1/V\left\langle \sum_{(i,j)} (x_{ij}^2/r_{ij})dv(r_{ij})/dr_{ij} \right\rangle$$

$$P_T = \langle\rho\rangle k_B T - 1/2V\left\langle \sum_{(i,j)} ((y_{ij}^2 + z_{ij}^2)/r_{ij})dv(r_{ij})/dr_{ij} \right\rangle$$

The integral is taken from a point in the bulk liquid x_l to a point in the bulk vapour x_v. The sums are over all pairs of molecules.

With potential parameters appropriate to an argon interface we obtained, $\gamma_{23} = 3\,\text{mN/m}$ in reasonable agreement with experiment ($\sim 5\,\text{mN/m}$ at 120 K). To calculate the surface tension of the curved interfaces γ_{13} and γ_{12} (Figs. 8, 11), special techniques [20] are required as the mechanical route described above is only straightforward [32] for a planar interface. In order to estimate the surface tension we calculate the work necessary to reversibly and isothermally increase/decrease the radius of the particulate by a certain amount (**dR**) in a fluid phase. The free energy associated with this virtual process is composed of a surface contribution from the expansion of the particulate surface area in contact with the fluid and a volume contribution

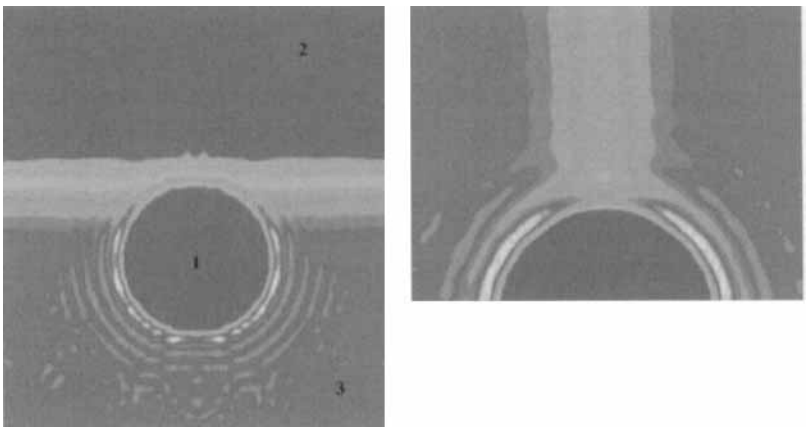

FIGURE 11 (a) the average L(**3**)V(**2**) interface (at $T^* = k_B T/\varepsilon_f = .75$) in the presence of a particulate (**1**): $\sigma = 10\sigma_f$. $\varepsilon = 1.85\varepsilon_f$. (b) the average LL interface ($T^* = 1.$), $\sigma = 10\sigma_f$, $\theta = 90°$. Colour coding: red-liquid density, blue-vapour densities (and particulate). (See Color Plate I).

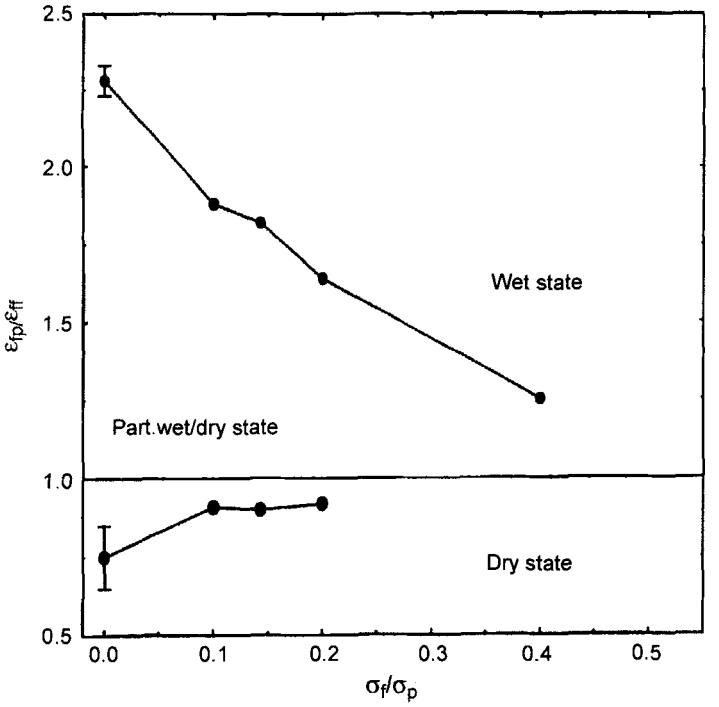

FIGURE 12 Wetting-drying boundaries [20] for the model defined in Figures 8 and 9.

from the work done against the bulk hydrostatic pressure P_b:

$$dF = (8\pi R_s\gamma)dR_s + 4\pi R_s^2 P_b dR_s \tag{1}$$

The forces are assumed to act at the radius of tension R_s, taken equal to the radius of the particulate. The change in free energy can be estimated in the canonical ensemble through the average:

$$\Delta F = -T^*\langle \exp\{-\beta[U(R') - U(R)]\}\rangle_R \tag{2}$$

where $R' = R \pm dR$ and U is the particulate energy. Putting $dF = \Delta F$ in Eqs. (1) and (2) we obtain the solid-fluid surface tensions γ_{12}, γ_{31}. Figure 13 below compares the contact angles predicted using these values in Young's equation with those found in the simulations, we find Young's equation is accurate for nanoparticulates, ≥ 3 nm. However the line tension (τ), may also influence the contact angle. We have estimated τ using

$$dF = [4\pi R(\gamma_{21}(1 + \cos\theta) + \gamma_{13}(1 - \cos\theta) - 0.5\gamma_{23}\sin^2\theta) + 2\pi\tau\sin\theta]dR + (4\pi R^2 P_b)dR \tag{3}$$

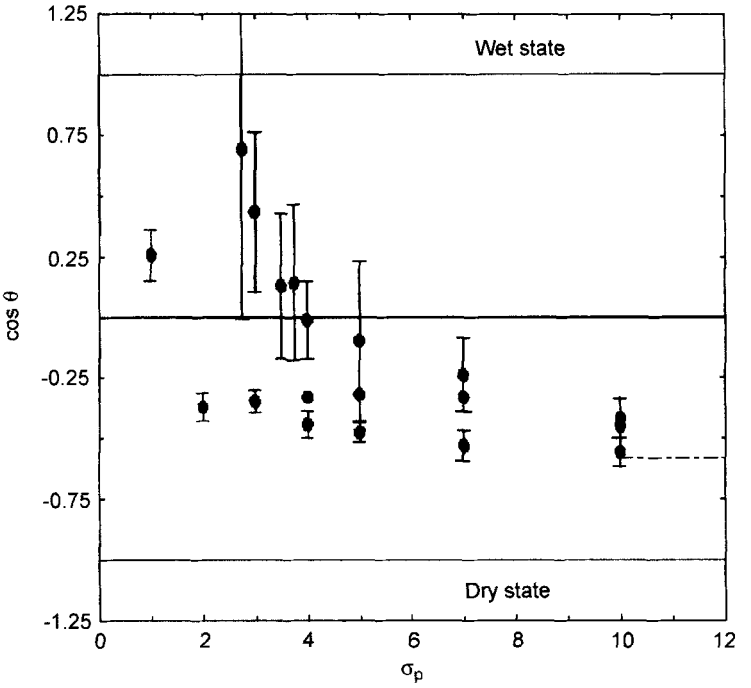

FIGURE 13 Contact angles [19] at the LV interface: circles from top of bottom, by simulation, theory including the line tension and theory without the line tension, at $T^* = 0.75$.

by calculating the free energy change of a particulate *in the interface*. Correcting Young's equation to take into account the line tension improves the agreement with the simulated contact angle. We also considered the case of a liquid–liquid interface (with $\gamma_{23} = 14\,\text{mN/m}$, Fig. 11b) where we found that Young's equation predicts wetting behaviour very accurately, even for diameters of just $\sim 1\,\text{nm}$. Figure 13 compares the simulated and predicted dependence of the contact angle on particulate size for a low surface tension interface (LV). Correcting Young's equation using the line tension improves the agreement and Young's equation seems to be accurate for nanoparticulates, $\geq 2\,\text{nm}$. As the particulate becomes smaller Young's equation breaks down. By analysing the corrected Young's equation and by performing simulations of higher tension interfaces it is possible to show that the contact angle only depends sensitively on the line tension when the fluid surface tension is low (as for the LV interface considered here $\gamma_{23} = 3\,\text{mN/m}$). For most water/air and oil/water interfaces ($\gamma_{23} = 50\,\text{mN/m}$), Young's equation may be used to accurately describe wetting at the nanoscale [21].

The line tension for the LV system discussed above is of the order of $\sim 10^{-12}$ N, whilst that for the LL system is $\sim 10^{-11}$ N. Experimental values for colloids of nanometer size are $\sim 10^{-11}$ N. Our predicted line tensions are in good agreement with experimental values at comparable interfacial tensions. We found that the line tension was a linear function of interfacial surface tension, confirming the theoretical predictions of Rowlinson and Widom [32].

An important technique for the investigation of colloidal properties is the measurement of surface pressure Π-area A curves for particulate assemblies at fluid interfaces. Having elucidated the properties of nanoparticles at infinite dilution we have been able to investigate directly the standard interpretation of the trough experiment by a) molecular dynamics simulation [24] (Fig. 14 shows a snapshot from a simulation of a monolayer at a liquid–liquid interface) and b) a free energy model [24, 25]. The monolayer consists of 16 colloidal particles of diameter ~ 3 nm. The interactions considered are of the short range Lennard-Jones type. The interaction strengths were adjusted so as to ensure the stability of the nanoparticulates at the interface avoiding the flocculation of the monolayer. The box dimensions were scaled such that the system density remains constant as in a real Langmuir-trough. At each surface area the surface

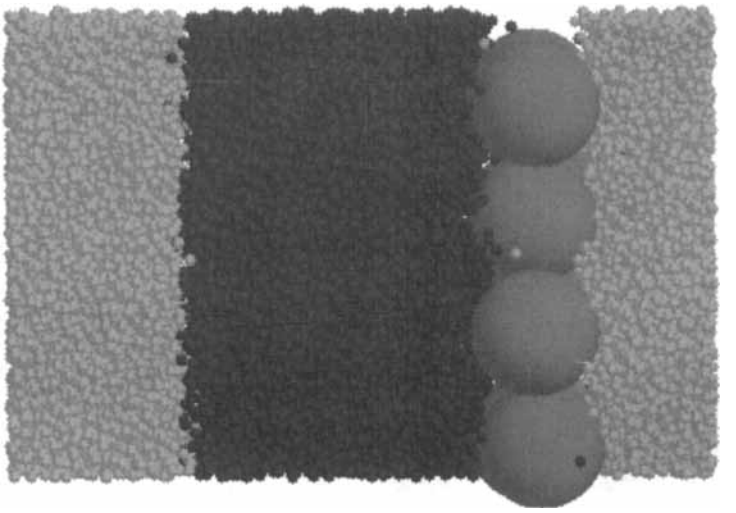

FIGURE 14 Simulation cell for the simulation of the pressure – area curve for nanoparticulates at a liquid–liquid interface. Red spheres represent nanoparticulates. The surface pressure is the difference in the surface tensions at the two interfaces (with and without particulates) [23, 24]. (See Color Plate II).

tensions of the two interfaces (pure and with the monolayer), and hence Π, were calculated. In Figure 15, Π increases rapidly as the layer compresses until the knee of the curve where the monolayer, now close packed in a hexagonal lattice, was expected to start to form a bilayer by ejecting particulates. However we observed instead that the interface buckled [22, 24, 25] (Fig. 16). These results have been validated by Langmuir trough experiments on micron sized particulates [25].

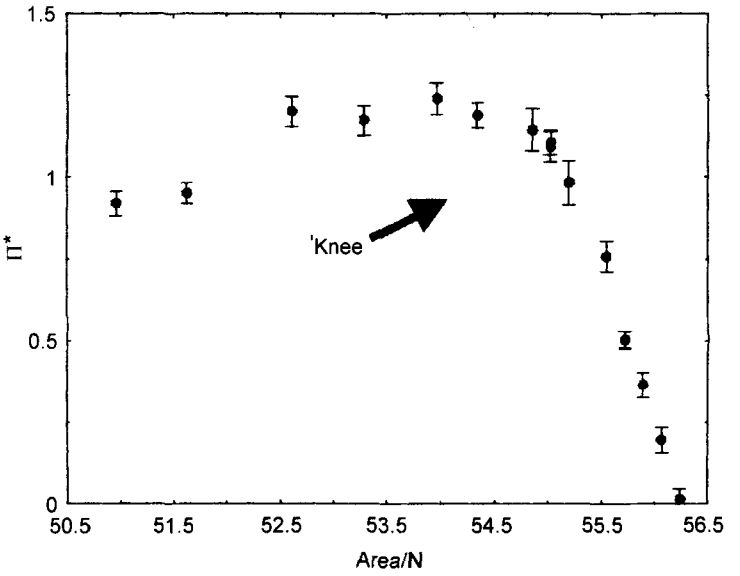

FIGURE 15 Preliminary results [23] for the surface pressure Π as a function of area per particle for a system of nanoparticles of diameter $8\sigma_{ff}$ showing the rise in pressure with decreasing area and the plateau at $\Pi = \gamma$ the liquid–liquid surface tension.

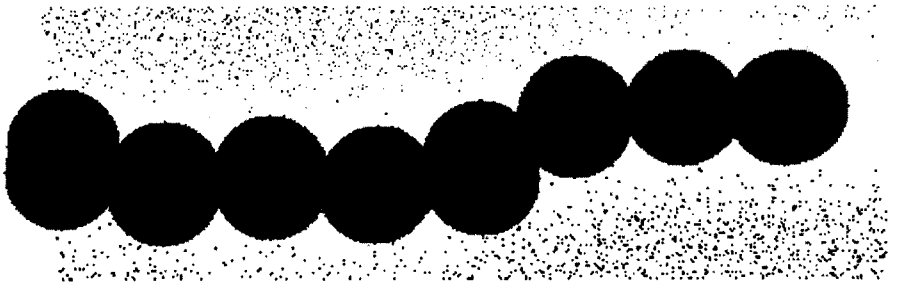

FIGURE 16 Snapshot from a molecular dynamics simulation [23, 24] showing the "buckling" mechanism. This was observed for monolayers with surface areas smaller than the "knee" surface area. The dots represent the fluid particles; the size was reduced for clarity.

4. INDUSTRIAL APPLICATIONS OF MOLECULAR MODELLING [33]

The continued prosperity of the UK chemical industry depends on the ability of its scientists and engineers to design and then produce, molecules and phases capable of performing specific tasks. For example, new pharmaceutical drugs, more specific herbicides, improved polymers for packaging, better additives for fuels, inhibitors for scale, corrosion and clay swelling, retarders for downhole cements, environmentally friendly fabric softeners. The range of molecules and applications is very wide. The faster and cheaper new molecules and materials can be brought to market the greater the likelihood of commercial success. Traditionally, molecules have been sought largely through experimental research with theory and modelling playing a relatively minor role. However developments in computer hardware and molecular modelling software in the last ten years have transformed modelling from an academic subject into a practical tool for molecular design. This change started in the pharmaceutical sector, where the use of molecular graphics and associated software has been successful in aiding drug design. The same methods are now having an impact more generally.

Industry requires chemical and physical data as well as an understanding of molecular processes for many reasons. It is convenient to group these needs into overlapping categories according to whether the need is to *create a* new *product* or to *improve* an existing *process* [34]. For the former the need is primarily to increase understanding at a molecular level to guide chemical intuition and to be able to screen candidate molecules, materials or phases prior to experimental verification; for the latter the need is for chemical and physical data (*e.g.*, heats of formation, rate constants, phase densities, transport coefficients, selectivity's *etc.*) for process and reservoir simulators.

For *product* innovation, information can be required at two levels. For many products, it is the properties of the *individual active molecules* that are of overriding importance. Examples include site specific drugs in the pharmaceutical industry, inhibitors to retard crystal growth for oil field applications (see the example of cement retarders in this section) or template molecules to modify or initiate zeolite crystal growth in the chemical industry.

In these examples, the desired effect occurs primarily as the result of the individual action of the active molecules acting at specific sites or on specific particles. In other circumstances, the industrial problem amounts to designing, optimising or selecting the overall properties of a *material or*

fluid phase. For this second type of design problem, the desired properties result from the collective response of the molecules. Examples include the design of solvents for paints or dry cleaning, as well as CFC replacements for refrigeration. The target properties will be a combination of appropriate bulk phase thermodynamics along with an acceptable health, safety and environmental response. Other fluids are designed to have special transport (*e.g.*, rheological) properties. Examples include some domestic cleaning fluids, where a thick consistency is required, or polymer melts that must be capable of extrusion and flow during processing. Collective properties are also important in designing the appropriate mechanical or optical response in materials such as polymeric pipes or packaging.

These two concerns; that of designing *new site-active molecules* or of tailoring the collective properties of *material or fluid phases* are not exclusive and often the final product will be formulated so that it contains both site-active and phase-active components. A good example is an oil field mud which must have the correct rheology while containing site active molecules concerned with, amongst other problems, controlling clay swelling and breakdown. Another is the problem of designing pharmaceutical tablets that dissolve (phase active) at the right time and in the right place in the body to deliver the drug molecule (site active) where it is needed.

Where molecular simulation is employed to provide information to assist in achieving goals in industrial or applied research it is unlikely to be used by itself. It is much more probable that it will be one activity in a larger programme which can include other modelling methods (electronic, molecular mechanics, bulk thermodynamics, structure-property, heat or mass transport). In addition there may be experimental and theoretical research programs which will influence, and be influenced, by the modelling. Approximate solutions to idealised models of complex systems still play an important role in guiding both molecular modelling and experiment.

The largest barrier to progress is often the incomplete characterisation of the (usually rather complex) real system. It can be difficult to obtain reliable information on the number and type of species present or the physical and chemical structure of the local environment. Modelling cannot proceed until the system is to some extent characterised and the characterisation itself can require input from modelling (for example the characterisation of microporous materials by gas adsorption or X-ray/neutron scattering). Finally there can be financial models which, depending upon the research results, will indicate whether the new product or process makes economic sense. All of these different elements will contribute to solving the problem at hand.

Table I lists several general types of modelling used in industrial research. Second column lists the basic units that are modelled. For instance at the bulk level, materials are assumed to be continuous. The objects modelled are infinitesimal elements of continuous solids or fluids. The third column states the fundamental equations which are solved to predict the properties (column four) of the specific physical models. A few examples of modelling software packages are given in column six. These lists are not complete and do not constitute a recommendation. As stressed above an industrial application is likely to involve modelling at many levels so that these examples are not exclusive. The results from modelling at one level can feed into modelling at a higher level of approximation. In order to emphasise the inter relatedness of industrial modelling, Figure 17 shows possible relationships between the different types of modelling.

In the following subsections examples of industrial applications in the chemical industry are presented. The discussion is focused on applications based on gas adsorption, polymer miscibility, and crystal growth. Applications to drug design are discussed in, for example, Refs. [35, 2].

TABLE I Examples of modelling techniques

Type of modelling	*Physical models (specific)*	*Basic equations (general)*	*Predicted properties*	*Example of application area*	*Examples of software*
Electronic (*Ab initio*, semi empirical)	Electrons Nuclei *Coulomb's Law*	Schrödinger Equation	Minimum Energies, Affinities, Structures, Charges, ...	Materials/ Drug design	CASTEP CRYSTAL DMOL GAUSSIAN SIESTA
Molecular (graphics, mechanics, dynamics) Monte Carlo	Molecules *Potential Functions (forcefields)*	Classical Equations of Motion/ Gibbsian Ensembles	Molecular Structures, Energies, Phase Behaviour, Dynamics	Materials/ Drug design	DLPOLY DLV GULP CERIUS2
Phenomeno logical	various	Applied Maths and Stats/ van der Waals Equation"	Solubility/ Phase equilibria (VLE, SLE, Miscibility, T_g, ...)	Materials/ Drug design	REKKER UNIQAC/ UNIFAC
Bulk (Continuum) (Thermo Dynamic, CFD, FE,)	Continuum Fluids *Constitutive Relations* $P(V, T)$, $\eta(\dot{\gamma})$	Laws of Thermo dynamics/ Conservation Equations	Phase Equilibria Heat, Mass Momentum Transfer	Process, Pipeline and Reservoir Simulation	FLUENT ASPEN-PLUS VIP

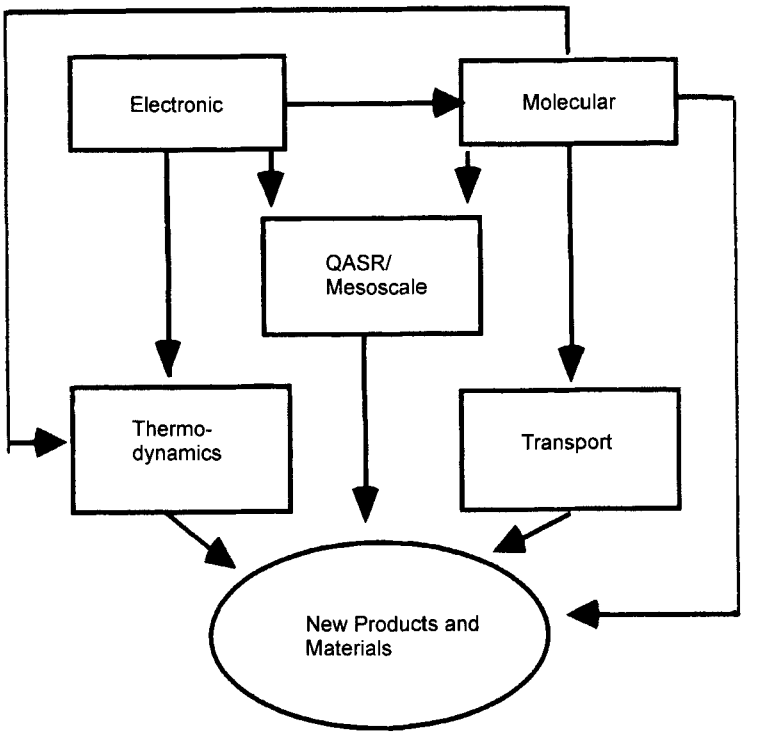

FIGURE 17 Possible relationships between different types of modelling.

4.1. Materials Design and Optimisation

The first example deals with the adsorption of methane in activated carbons; these are graphitic microporous solids obtained by carbonising starting materials, such as polymer resins or coconut fibres, and activating them, *i.e.*, opening up the microporosity by chemical attack. They are able to adsorb considerable quantities of gases and are used as adsorbents in separation processes and as catalyst supports. They are also of interest to a number of companies worldwide as potential storage materials for methane powered vehicles. In 1984 experimental investigations at the BP research laboratories found that a carbon activated with molten alkali could adsorb unusually high amounts of methane. This led to the formulation of a novel idea for gas transportation from natural gas fields, namely to adsorb the gas directly onto activated carbon beds in special container ships at relatively low pressures. In this way the high capital costs of liquefaction plants could be avoided. Initial studies indicated

that the scheme might allow small remote gas fields to be commercially exploited.

The key factors that determined the projects viability were; the carbon performance (how much natural gas could be transported on the carbon), the carbon manufacturing costs, the gas loading terminal costs, the ship volume and costs, and the shipping cycle parameters which include elements such as ship turn around time (this in turn would depend on the distance over which the gas was to be shipped). In addition there were other factors outside the control of the project such as the projected selling price of gas. A number of different teams were involved in supplying models and data for each of these factors which were incorporated into a financial spreadsheet. The spreadsheet was used to predict the discounted cash flow arising from the project. If it was positive then there would be more cash in the future (discounted back to the project start date) as a result of the project going ahead than there would be if the project was abandoned. In this way the cash flows from different methods of transportation (liquefied natural gas, pipelines, adsorption) could be compared.

As noted above one key factor in the project was the performance of the carbon. It became clear that the project was unattractive compared to the alternatives at the experimental gas (methane) loadings. However if the carbon could be improved to adsorb more methane then there could be circumstances in which it would be an attractive option. The crucial unknown quantity was the amount of methane (and methane/ethane mixtures) which would be adsorbed by an optimised carbon material. Since such a material had not yet been made, the adsorption could not be measured.

Only molecular simulation was able to reliably predict for model carbons the methane adsorption as a function of micropore width, temperature and pressure. A study using grand canonical Monte Carlo simulation of the variation of methane uptake in graphitic pores was carried out at the proposed operating conditions (-30 C and 3.5 MPa).

Figure 18 below shows that there is an optimum pore width H, defined as the distance across the pore between the carbon nuclei forming the walls, at 11.43 Å for these conditions (other results included the variation of the optimum pore size with temperature and pressure). Therefore if all the void volume in the carbon could be concentrated at constant total void volume in a narrow range of pore sizes around 11.43 Å the material would provide an optimum performance for methane adsorption. Similar simulations were carried out for methane–ethane mixtures, which showed the expected preferential adsorption of the ethane. This data produced an estimated

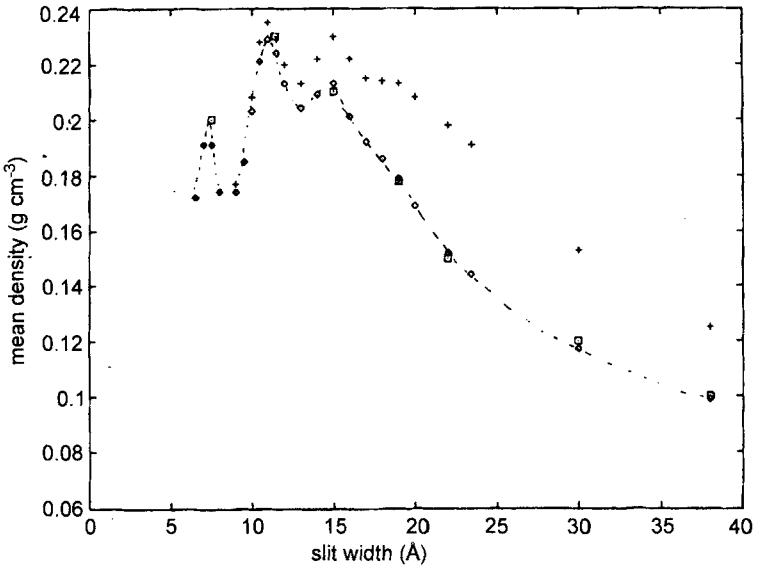

FIGURE 18 Plot of the mean density of methane in graphitic pores at −30 C and 3.5 MPa as predicted by simulation (squares) and non local density functional theory (diamonds, with cut off of 2.5 methane sigmas, crosses) showing the optimum pore sizes.

methane optimum uptake of 0.5 g of gas per gram of carbon at the specified operating conditions. Lowering the temperature increased the uptake but also increased the project costs.

The simulations allowed the financial model to be used to calculate the project economics in the event that the lab (perhaps after considerable investment in staff and equipment) was able to produce the best possible carbon. It showed that except for a narrow range of conditions the existing technologies were superior and the project was abandoned. Thus the new ability provided by grand canonical Monte Carlo simulation to predict accurate results for *idealised* model materials had been instrumental in stopping a major project which might otherwise have continued at considerable cost, and which for the materials and applications considered at the time would not have produced a usable material.

The modelling component of the project required about 6 months to write the software and generate the data (including many not discussed here) at a cost of approximately $70,000. The exact financial benefit is difficult to judge since it involves an estimate of the length of time the experimental work would have continued in the absence of the modelling results. Assuming an extra year of work the savings were of the order of half a million dollars.

An unanticipated spin off from this work was the development of a novel characterisation method for microporous materials [36]. The development of new activated carbons for gas transportation highlighted the need for an accurate characterisation of their microstructure. The standard experimental characterisation method, nitrogen gas adsorption, was hampered by an inadequate analysis of the resulting isotherms. Molecular simulation data for model graphitic pores was used to test an approximate theory (local density functional theory) which was then used to generate a database of model isotherms. When combined with a simple model of the micropore geometry the database made possible an improved analysis of the experimental gas adsorption data resulting in more reliable pore size distributions and information on pore connectivity. Subsequent work has led to improved versions [37, 38].

Simulation of adsorption phenomena in industry is not limited to carbons. A group at Air Liquide in France [39] have used grand canonical Monte Carlo simulations of adsorption isotherms to rationalise N_2/O_2 selectivities on zeolites such as LiY and NaY. They have been able to link microscopic data such as molecular interactions and zeolite crystal structures to macroscopic observables such as separation factors as a function of temperature and pressure. One benefit of such an approach is that it allows the researcher to quickly describe the possible limits of experimental synthesis programs designed to produce more effective materials for gas separations. Indeed the Air Liquide group stress the importance of modelling in guiding their experiments.

4.2. Polymer Miscibility

The previous application illustrated how molecular simulation can be used to calculate experimentally inaccessible data and how such data can be used to influence the planning and evaluation of industrial research projects. In this section the use of molecular simulation to predict data that could easily be measured will be discussed. In this case molecular simulation and molecular modelling can produce dramatic improvements in research efficiency by allowing far fewer experiments to be carried out to reach the same goal. The application is the computer-assisted selection of polymers for high performance polymer blends by a modelling group at Hoechst Celanse [40]. The example demonstrates the inter-relatedness of modelling methods illustrated in Figure 17. The Hoechst Celanse team used electronic, energy minimisation and molecular simulation methods to construct a 'structure-property' relationship (more accurately an "intermolecular

energy-condensed phase property' relationship) to predict polymer miscibility. Such an approach has wider application, for example, in predicting the mixing and demixing of surfactants in solution.

Polymeric materials have a wide variety of industrial uses from food packaging, to gas pipelines. The necessary materials properties can be achieved by blending different polymers, each component contributing a particular attribute, for example high strength, or permeability. However in order to achieve a satisfactory product it is important that the various components mix properly. This is most easily ensured if the blended polymers form a single phase *i.e.*, they are miscible. Therefore it is vital to test potential blends for miscibility early in the research program. This can present a considerable challenge as the number of different mixtures can grow very rapidly. For n pure component polymers there are $n(n-1)/2$ possible binary mixtures, most of which can be expected to be immiscible and therefore not candidates for the final material. Since a modest research programme might involve 25 resins and a typical screening experiment on one pair takes 3 weeks (involving a researcher, technician and analytical support) the Hoechst team estimated that the screening of the binary mixtures could take up to 18 years to complete. Clearly although, in principle, the information could be obtained, in practice the screening could not be completed unless some form of reliable prescreening of the mixtures could be carried out.

Previous work, both experimental and theoretical, has suggested that polymer miscibility is largely controlled by local segment–segment interaction energies. In this case the miscibility can be described by the excess energy of mixing which is essentially the energy difference between like ($a-a$ and $b-b$) and unlike pairs ($a-b$) of polymer molecules; $\Delta E_{ab} = E_{ab} - 0.5(E_{aa} + E_{bb})$. When this energy difference is negative, misciblity is predicted.

Jacobson *et al.* [40] made the further assumption that this energy difference could be calculated in vacuum for short chains consisting of about 200 atoms describing 3–6 repeat units. As indicated in Figure 17 a number of modelling options are available to calculate the molecular level properties that form the basis of such structure–property relationships, including quantum mechanical packages as well as force field approaches used in molecular mechanics and molecular simulation codes. Jacobson *et al.*, used a combination of commercial modelling packages including self consistent field (SCF) quantum codes and molecular mechanics (energy minimisation), and molecular dynamics to prepare short polymer segments in low energy configurations. The pair energies were obtained by 'docking' one fragment

onto another (in this case with static fragments) in order to obtain the lowest possible pair binding energy from which the energy differences ΔE_{ab} were computed.

The accuracy of the approach (which, after all, rests on some quite severe approximations) was tested by examining blends of poly [3,5-dimethylphenylene oxide], PPO, with copolymers of *ortho-* and *para*-chlorostyrene for miscibility and then comparing with experiment. Good agreement was obtained. Following this success, the procedure was applied to the evaluation of the miscibility of high performance polymers and used to eliminate blending pairs with high positive values of ΔE_{ab} from the experimental screening programme. Jacobson *et al.*, state that 'We are not aware of any inconsistencies in our predictions in the many cases where experimental confirmation of either miscible or immiscible pairs has been carried out'. The modelling study was able to reduce the number of blending pairs from 300 to 30 in four months running concurrently with the experiments. This represents a considerable reduction in research costs.

The methodology used in these studies was improved and extended by Tiller and Gorella [41]. They calculated ΔE_{ab} for a miscible (polyethylene oxide 'PEO', polyacrylic acid 'PAA') and an immiscible pair (polyethylene oxide, polypropylene 'PP') in great detail, looking at the effect of polymer segment length, cut offs and extent of conformational search. They find the method to be a reliable indicator of miscibility even using quite short segments.

Jacobson *et al.*, state that the payback of molecular modelling is typically 4 dollars for each dollar spent. The benefits of using molecular modelling as a tool to prescreen materials in order to dramatically reduce the number of experiments required in an industrial research project come both from the direct financial savings and also from the ability to explore many more possibilities than would otherwise be the case.

4.3. Molecular Design

The previous examples have dealt with the design of adsorbent materials and the screening of polymeric mixtures for miscibility *i.e.*, with phase active molecules. This subsection considers an industrial application involving the design of site active molecules as inhibitors for downhole cement. The use of molecular modelling tools to design molecules to block active sites is common in the pharmaceutical industry. As we shall see below there are now good examples of the same approach in oil field chemistry.

Cements are used in the oil field to fix steel casings to formation rock in oil well boreholes to prevent them collapsing and to act as seals. Since the cement must be pumped to the bottom of boreholes that can be thousands of feet deep and will encounter large variations of pH, temperature and shear, cement properties such as setting time must be strictly controlled. As cement is a complex, poorly understood material, control has been largely based on empirical knowledge. For an oil field service company, the ability to reliably tailor setting times gives a commercial advantage when bidding for work. A group at Schlumberger Cambridge Research [42] used computational chemistry tools to understand the mechanism of cement inhibition and then have gone on to design and test new inhibitors.

Any attempt to apply computational chemistry to the full problem would fail due to the time scale of the problem and the complexity of the material. Instead the rate determining step must be found within the simplest possible model. Coveney *et al.* [42] proposed a chemical clock model in which the formation of ettringite (see below) crystal from ettringite gel was the key step. Ettringite gel formation by hydration occurs as soon as the cement comes into contact with water causing the initial rise in cement viscosity before the plateau period. The gel covers the silicate grains with an impermeable coating which prevents silicate hydration and delays the formation of percolating silicate gel bridges and the final setting of the cement. The transformation of the ettringite gel into its crystalline form at the end of the plateau period allows water to reach the silicate grains and hydrate them leading to silica gel bridges between grains, structural percolation and setting. Within this simple model of cement setting if the crystal growth can be inhibited then the setting time will be increased and *vice versa*.

Phosphonates are known cement inhibitors. In order to rationalise their behaviour Coveney *et al.*, used semi-empirical quantum mechanical codes together with energy minimisation and molecular dynamics to investigate the behaviour of phosphonate molecules at the fastest growing face of ettringite crystals (the 001 face). They found that the phosphonate groups were isoelectronic and isosteric with the sulphate groups in the 001 ettringite surface and postulated that they replace sulphate in the growing crystal, poisoning these growth sites and inhibiting crystal growth leading to the retardation of cement setting. By considering the number, position and flexibility of phosphonate groups in phosphonate retarders with respect to the 001 ettringite surface Coveney *et al.*, were able to rank the molecules in terms of effectiveness in agreement with experiment. They went on to design new long chain and cyclic retarders which when synthesised have been found to be very effective.

5. CONCLUSIONS

In section four the role of computational chemistry in industrial research has been considered. Computational chemistry techniques have been placed in the context of the wide range of modelling tools now available. The case histories have demonstrated their use in (i) understanding key microscopic mechanisms and linking them to macroscopic behaviour, (ii) calculating the properties of perfect materials and being able to estimate the possible 'stretch' in existing materials, and (iii) screening molecules and phases for desirable properties, helping to reduce the number of experiments.

The use of computational chemistry to fill QSAR and other databases will become increasingly important in the future. The rate at which these new procedures spread will be determined to a large extent by how quickly they can be made available to less experienced users. As the speed of calculation increases due to faster computers, parallelisation and more efficient algorithms, the amount of data to be handled could very quickly become difficult to manage. Increasingly the management, storage and analysis of such data will need to be automated. It is quite probable that the calculations themselves will be performed remotely *via* an intranet or the internet. Such 'active' databases are already being developed by commercial software companies. Molecules are placed into a spreadsheet either from a graphical user interface or read in from a database of previously calculated results. Properties are specified for each molecule in the table based upon a particular computational procedure. The properties are then either retrieved from the database, if they have already been calculated, or they are obtained by launching the appropriate calculations from the spreadsheet. Once the calculations are finished the table and database is updated and subsequent analysis can be performed. It may be that active databases provide the key to a modelling version of combinatorial chemistry where a huge number rapid, automatic calculations would be used to screen very large numbers of mixtures of molecules or phases for a desirable properties.

Another challenge for the future is to integrate the use of molecular level simulation into the modelling and prediction of the properties of materials where the desired properties, be they electronic, optical, magnetic, chemical, thermal or mechanical, may be determined at the electronic, atomic, microstructural (< 100 nm) or mesostructural ($\sim$ microns) level and by interactions between these different scales. Figure 17 gave an example of some of the links between different modelling techniques appropriate to the chemical and petrochemical industries; the need to take into account the role

of micro and meso structures in determining the properties of structural materials such as alloys, synthetic polymers and their blends, composites and coatings, introduces another order of magnitude of complexity into the modelling process. This challenge can only be met by new and improved modelling tools (*e.g.*, quantum molecular dynamics, coarse graining and mesoscale procedures) and hardware developments.

Acknowledgements

I thank Dr. F. Bresme and Mr. N. Fenwick for their collaboration on the nanoparticle problems described in this article. Figures 10 and 12 are reproduced by permission of the American Physical Society, Figure 13 with permission of the American Chemical Society.

References

[1] See for example Sambursky, S. (1956). "The Physical World of the Greeks", Princeton University Press.
[2] Leach, A. R., 'Molecular modelling principles and applications', Longman, 1996.
[3] Metropolis, N., Rosenbluth, A. W., Rosenbluth, M. N., Teller, A. H. and Teller, E. (1953). 'Equation of state calculations by fast computing machines', *J. Chem. Phys.*, **21**, 1087.
[4] Rosenbluth, M. N. and Rosenbluth, A. W. (1954). 'Further results on Monte Carlo equations of state', *J. Chem. Phys.*, **22**, 881.
[5] Wood, W. W. and Jacobson, J. D. (1957). 'Preliminary Results from a Recalculation of the Monte Carlo Equation of State of Hard Spheres', *J. Chem. Phys.*, **27**, 1207.
[6] Alder, B. J. and Wainwright, T. E. (1957). 'Phase Transition for a Hard Sphere System', *J. Chem. Phys.*, **27**, 1208.
[7] Wood, W. W. and Parker, F. R. (1957). 'Monte Carlo Equation of state of molecules interacting with the LJ's potential: 1 A supercritical Isotherm at about twice the critical temperature', *J. Chem. Phys.*, **27**, 720.
[8] Alder, B. J. and Wainwright, T. E. (1959). 'Studies in Molecular Dynamics I General Method', *J. Chem. Phys.*, **31**, 459.
[9] Gibson, J. B., Goland, A. N., Milgram, M. and Vineyard, G. H. (1960). 'Dynamics of radiation damage', *Phys. Rev.*, **120**, 1229.
[10] Rahman, A. (1964). 'Correlations in the motion of atoms in liquid argon', *Phys. Rev.*, **136**, 405.
[11] Sadus, R. J. (1999). Molecular Simulation of Fluids: Theory, Algorithms and Object Orientation, Elsevier, Amsterdam, 1999.
[12] Allan, M. P. and Tildesley, D. J. (1987). *Computer Simulation of Liquids*, Clarendon Press.
[13] Garrod, C. (1995). *Statistical mechanics and thermodynamics*, OUP.
[14] See *e.g.*, Smit, B. and Frenkel, D. (1996). *Understanding Molecular Simulation: From Algorithms to Applications*, Academic Press.
[15] Gould, I. R., 'Computational Chemistry: Application to Biological Systems', *Molecular Simulation* (this issue).
[16] Boghosian, B. M., Coveney, P. V., Love, P. and Maillot, J.-B., 'Mesoscale Modelling of Amphiphillic Fluid Dynamics', *Molecular Simulation* (this issue).
[17] Nicolaides, D., 'Mesoscale Modelling', *Molecular Simulation* (this issue).
[18] Drukker, K. (1999). 'Basics of Surface Hopping in Mixed Quantum/Classical Simulations', *J. Comp. Phys.*, **153**, 225.

[19] Bresme, F. and Quirke, N. (1998). 'Computer Simulation Study of the Line Tension of Nanometer Sized Particles at Liquid–Vapour Interfaces, *Phys. Rev. Letts.*, **80**.
[20] Bresme, F. and Quirke, N. (1999). 'Computer Simulation of Wetting and Drying of Solid Particulates at a Liquid Vapour Interface', *J. Chem. Phys.*, **110**, 3536.
[21] Bresme, F. and Quirke, N. (1999). 'Nanoparticulates at Liquid–Liquid Interfaces', *Physical Chemistry Chemical Physics*, **1**, 2149.
[22] Bresme, F. and Quirke, N. (2000). Computer Simulation of Liquid Lenses at a Liquid–Liquid Interface', *J. Chem. Phys.*, **112**, 5985.
[23] Fenwick, N., *Ph.D. Thesis*, University of Wales Bangor.
[24] Fenwick, N., Bresme, F. and Quirke, N. (submitted).
[25] Aveyard, R., Clint, J. H., Nees, D. and Quirke, N., 'Structure and collapse of particle monolayers under lateral pressure at the octane/aqueous surfactant solution interface', *Langmuir* (in press).
[26] Turner, A. and Quirke, N. (1998). 'A Grand Canonical Monte Carlo Study of Adsorption on Graphitic Surfaces with Defects', *Carbon*, **36**, 1439.
[27] *E.g.*, Maddox, M. W., Gubbins, K. E. and Quirke, N. (1997). 'A Molecular Simulation Study of Pore Networking Effects', *Molecular Simulation*, **19**, 267.
[28] Nicholson, D., Cracknell, R. and Quirke, N. (1997). 'A Transition in the Diffusivity of Adsorbed Fluids Through Micropores', *Langmuir*, **12**, 4050.
[29] Sokan, V., Nicholson, D. and Quirke, N. (2000). 'Phonon spectra in model carbon nanotubes', *J. Chem. Phys.*, **113**, 1.
[30] *E.g.*, Callaway, M., Tildesley, D. J. and Quirke, N. (1994). 'Reordering of Surface Phases During Atomic Force Microscopy: A Simulation Study', *Langmuir*, **10**, 3350.
[31] Aveyard, R., Clint, J. H. and Nees, D. (1997). Theory for the determination of line tension from capillary condensation, *JCS Faraday Trans.*, **93**, 4409.
[32] Rowlinson, J. S. and Widom, B., *Molecular theory of capillarity*, Oxford Science, 1989 (Chapter 8).
[33] Some of the material in this section appeared in Ref. [34].
[34] Gubbins, K. E. and Quirke, N., '*Molecular Simulation and Industrial Applications: Methods, Examples and Prospects*', Eds. Gubbins, K. E. and Quirke, N., Gordon and Breach Publishers, 1996.
[35] Leach, A. R. and Green, D., 'Computational Chemistry in Lead Identification, Library Design and Lead Optimisation', *Molecular Simulation* (this issue).
[36] Walton, J. P. R. B. and Quirke, N. (1989). *BP Report* (PEB/01/86) January, 1986. Published In: Seaton, N. A., Walton, J. P. R. B. and Quirke, N., *Carbon*, **27**, 853.
[37] Lastoskie, C. M., Gubbins, K. E. and Quirke, N. (1993). Pore size distribution analysis of porous carbons, *J. Phys. Chem.*, **97**, 4786.
[38] Scaife, S., Kluson, P. and Quirke, N. (2000). Characterisation of porous materials by gas adsorption, *J. Phys. Chem. B*, **104**, 313.
[39] Mellot, C. and Lignieres, J. (1996). *Molecular Simulation*, **18**, 146.
[40] Jacobson, S. H., Gordon, D. J., Nelson, G. V. and Balazs, A. (1992). Miscible polymer blends: Local interaction energy theories and simulations, *Adv. Materials*, **4**, 198.
[41] Tiller, A. R. and Gorella, B. (1994). Estimation of polymer compatibility from molecular mechanics calculations, *Polymer*, **35**, 325.
[42] Billingham, J. and Coveney, P. V. (1993). Simple chemical clock reactions: Application to cement hydration, *J. Chem. Soc. Faraday Trans.*, **89**, 3021.